



# Buckling Behavior of Nose Cone Type Steel Tanks Including Horizontal Imperfection

Mahmut Kılıç<sup>1</sup>

Received: 18 December 2019 / Accepted: 4 July 2021 / Published online: 7 July 2021  
© Korean Society of Steel Construction 2021

## Abstract

Cylindrical shells have long been used as storage tanks in small or large sizes to store a variety of materials such as petroleum and derivatives. The radius to thickness ratios of these shells are classified as 1000 and 2000 according to which designers and international codes are attracted to the buckling due to their collapse in buckling. Considerable research has been conducted on cylindrical reservoirs under the influence of a hydrostatic force or an internal vacuum. Due to the low wall thickness of the shell structures, it is possible to cause any deformation and disturbance on the wall surfaces. Due to a variety of errors during construction or assembly, the designed tanks are not ideally constructed and have some geometric error. Horizontal imperfection caused by continuous welding on the steel sheet's edge to form the nose cone is the main concern of this work. The present paper attempts to discuss seven laboratory specimens under uniformed hydrostatic pressure with the 4t, 6t, 8t, 10t, 14t and 24t depths. The results revealed that there is a descent agreement between the results of the experiments conducted here and international codes and theories concerning with initial and overall buckling and collapse.

**Keywords** Horizontal imperfection · Steel tanks · Experimental · Buckling · Uniformed hydrostatic pressure · Nose cone

## 1 Introduction

Thin-walled shells are one of the building blocks of industries found in the world around us. One of these types of structures that is widely used in oil refineries is steel tanks that are designed and operated cylindrically. From a geometrical point of view, these tanks have a very low thickness compared to the other two dimensions and thus are classified as thin-walled structures and associated conditions. Buckling of tanks containing liquids is possible under different conditions and modes. Among the important issues in thin-walled shells are the occurrence of geometrical imperfections and their diminishing effects on the buckling capacity, buckling behavior and postbuckling of these structures. Due to the low wall thickness of the shell structures, it is possible to cause any deformation and disturbance on the wall surfaces. The buckling behavior is related to the critical load capacity, and the postbuckling behavior is related to the behavior of the structure after passing the load from the critical load to

the collapse stage. The critical load capacity of the shells under external pressure loads depends on two thin ratios of length to radius ( $L/R$ ) and radius to thickness ( $R/t$ ). Due to the significant change in the shell geometry at the buckling load, it is necessary to determine the postbuckling behavior until the complete collapse stage. Several factors influence the behavior of thin-walled structures, the most important of which are geometrical imperfections, loading, boundary conditions, and physical properties of materials. Among these factors, geometrical imperfection and loading are of particular importance. Geometric imperfections and loading must be considered to obtain a realistic estimation of the buckling capacity of the shells. Experimental studies show that the buckling load of a perfect shell (without geometry imperfection) is substantially different from the buckling load of the same geometrically imperfect shell. Stability analysis of thin-walled shells under external pressure load is one of the first requirements of the design. Due to the complex effect of potential forces during external pressure phenomena, the mere use of theoretical analysis can lead to lower or higher estimates being true. Therefore, experimental studies have a valuable place in this context. In the past two decades, Showkati and his colleagues experimented with cylindrical and cone reservoirs under uniform hydrostatic loading and

✉ Mahmut Kılıç  
mahmut.kilic@atauni.edu.tr

<sup>1</sup> Department of Civil Engineering, Engineering Faculty,  
Ataturk University, 25030 Erzurum, Turkey

axial forces. Showkati and Ansourian (1996) verified the initial confirmation of the support position on the buckling of tiny vessels of a small cylindrical slab. In contrast, Aghajari (2006) studied the buckling of cylindrical tanks under hydrostatic loads with different wall thicknesses. In turn, Showkati and Shahandeh (2009) showed that two factors (ring stiffeners and stringers) are important for the capacity of cylindrical tanks to buckle. Showkati and colleagues also studied the buckling of conical reservoirs (Ghazijahani & Showkati, 2011; Ghazijahani & Zirakian, 2014; Golzan & Showkati, 2008; Maali et al., 2012; Niloufari et al., 2014). During the past 10 years, Ghanbari Ghazijahani and his colleagues conducted many experiments on cylindrical tanks. Most of their experiments focused on the imbalance created on shells and the buckling effects on these shells (Ghazijahani et al., 2014a, 2014b; Ghazijahani et al., 2015a, 2015b; Ghazijahani et al., 2015). Ghanbari Ghazijahani and his colleagues also examined the effects of localized dents on thin-walled structures (Ghazijahani et al., 2014c). Recently, Maali et al. (2019) investigated the effects of buckling behavior on localized dents on cylindrical and conical thin-walled shells. Experiments were performed on the produced samples. The present study investigated seven specimens under uniform external pressure. One specimen was the perfect model, without geometry imperfection, with the remaining specimens having imperfections with amplitudes of 4t, 6t, 8t, 10t, 14t, and 24t (for the labeling of all specimen tests, A is the horizontal depth and width imperfection on the cone, and t is the thickness of the steel tank shell). Hence, the purpose of this study was to investigate the effect of horizontal rolling line imperfections on the buckling and postbuckling behavior of nose cone-type steel tanks, but horizontal rolling line imperfections occurred on the cone shell. Herein, horizontal imperfection was introduced at different depths and widths around the conical shells in the steel tanks. Each specimen was compared to other specimens based on the initial buckling, overall buckling, and collapse, in accordance with theoretical formulas. Finally, the reversal method and the buckling waves are presented in accordance with the

relevant theory. The difference between theory and dented experiments, what has to be, as a result of non-theoretical behavior of dented samples. However, we tried to make a connection between theory and dented ones.

## 2 Testing Process

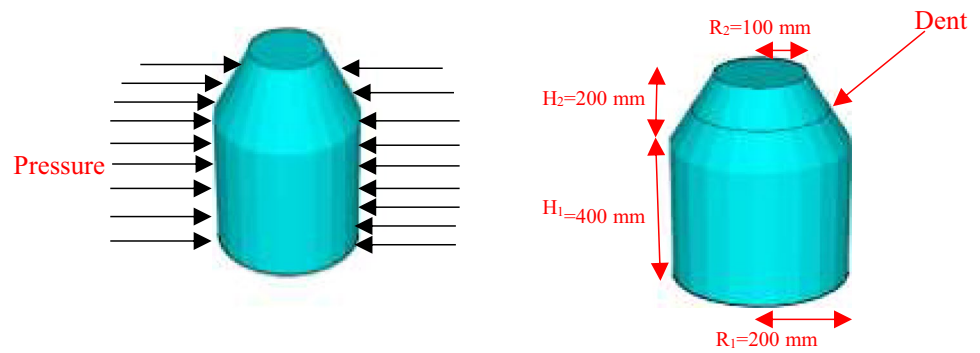
Seven models of nose cone-type steel tanks are investigated under uniform external pressure. The experimental size models were selected by various issues. Primarily, model geometries were limited to laboratory conditions. Second, the radius to thickness ratios (R/t) of cylindrical shells are classified within the stage of 300–1000 according to the experimental designers (Fatemi et al., 2013; Golzan & Showkati, 2008). Finally, the imperfections on the models selected by a realistic size depended on the thickness of the cylindrical wall. The details of the models are given in Table 1 and Fig. 1. The joint between the conical and cylindrical parts of the nose cone-type steel tank is one of the most important parameters for buckling capacity. This concern is also related to the results of the great influence of the junction and the high possibility of warping. Because of this issue, a ringing stiffener was used between the cylindrical wall and the conical roof. Solder was used instead of welding to attach the roof to the cylinder wall body.

The aim of the study was horizontal imperfection at different depths and widths around the conical shells in the steel tanks. The model names are At, where A defines the horizontal depth and the width of imperfection, and the thickness of the shell is defined as t. The imperfections are designed as the parameters of thickness and labeled 4t, 6t, 8t, 10t, 14t and 24t. The sample thickness was 0.45 mm, and the height to radius ratio was 2 ( $H/R=2$ ) (H is the height of the cylinder, and R is the radius of the cylinder). The tensile properties of the steel models are obtained according to relevant standards. The average failure stresses and yield strengths were 303.55 MPa and 181.42 MPa, respectively.

**Table 1** Initial geometry of test specimens

Specimen	R <sub>1</sub> (mm) cylinder	R <sub>2</sub> (mm) conical	H <sub>1</sub> (mm) cylinder	H <sub>2</sub> (mm) conical	t (mm) cylinder	t (mm) conical	Dent width (mm)	Dent depth (mm)	Dent location
Perfect model	200	100	400	200	0.45	0.45	–	–	H <sub>2</sub> /2
4t	200	100	400	200	0.45	0.45	1.8	1.8	H <sub>2</sub> /2
6t	200	100	400	200	0.45	0.45	2.7	2.7	H <sub>2</sub> /2
8t	200	100	400	200	0.45	0.45	3.6	3.6	H <sub>2</sub> /2
10t	200	100	400	200	0.45	0.45	4.5	4.5	H <sub>2</sub> /2
14t	200	100	400	200	0.45	0.45	6.3	6.3	H <sub>2</sub> /2
24t	200	100	400	200	0.45	0.45	10.8	10.8	H <sub>2</sub> /2

**Fig. 1** Details of the experimental test model



The Young's modulus was 190 GPa, and the Poisson's ratio was 0.28.

Rolls were formed by a roll machine after cutting the plates. Then, the ends of the cylinder were soldered to each other to form the elements. In the same way, the conical part was cut from the plates, and rollers were formed by a roll machine. Before joining the ends of the conical element, the dent was given with the help of the machine, as shown in Fig. 2. The desired dent can be given by changing the machine parts. After the necessary parts are installed, they are passed through the machine, and the dent is given. Dent elements are shown in Fig. 2. The ends of the conical element were joined after the dents were introduced. Then, the cylinder and conical element were brought together and combined.

-The installation of laboratory models is as follows:

After the sample was placed in the test instrument, the upper and lower hood parts were filled with silicone. In this case, the sealing was ensured.

The upper head was placed with the help of a crane. The bolt shown in Fig. 3 was closed so that the weight of the hood did not enter the sample. Thus, the head load was carried to the bolts and crane.

A Zinisan brand vacuum pump with 600-kPa hydrostatic pressure capacity was used. A 600-kPa pump is used for

the external pressure, and this pump supplies the load as a control. Additionally, a load cell vacuum pump was used to bake the load. Six nuts were used to control external load. Figure 3 provides an image of the six nuts. Additionally, an extra crane was used to control the external load. Data collections were made by using a datalogger. The vertical displacements were measured at  $0^\circ$  and  $180^\circ$  at different elevations ( $H/2$ ) on the cylindrical shell and  $90^\circ$  at different elevations ( $H/2$ ) for the cone by using three LVDTs (linear variable differential transformers). The LVDT transducers were used and coded as D1, D2, and D3. These three LVDTs (SDP-300, Japan) were 300 mm in length. The measurement error of the LVDT was 0.001 mm (Sagiroglu, 2018). Throughout the experimental work, all LVDTs were connected to prevent magnetization from overturning to the base. In all experiments, two strain gauges (YEFLA-5) were installed (S1 = horizontally on the cylindrical shell and S2 = vertically on the conical shell) (Fig. 3). All strain gauges were installed in the  $H/2$ . Table 2 lists the degrees of their locations. Before installing the strain gauge, they were placed carefully with a flap. After cleaning their contact areas, a special adhesive was used to immobilize them on the desired location. Their resistance was  $121 \Omega \pm 0.5\%$ , the sensitivity coefficient was  $2.1 \pm 2\%$ , and their sizes were  $3 \text{ mm} \times 5 \text{ mm}$ .

**Fig. 2** Details of the dent machine

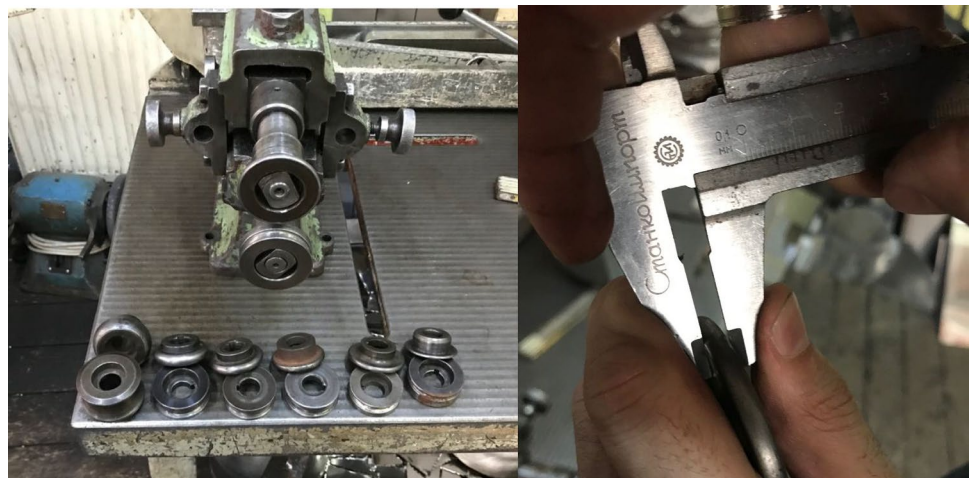


Fig. 3 Detail of a test specimen

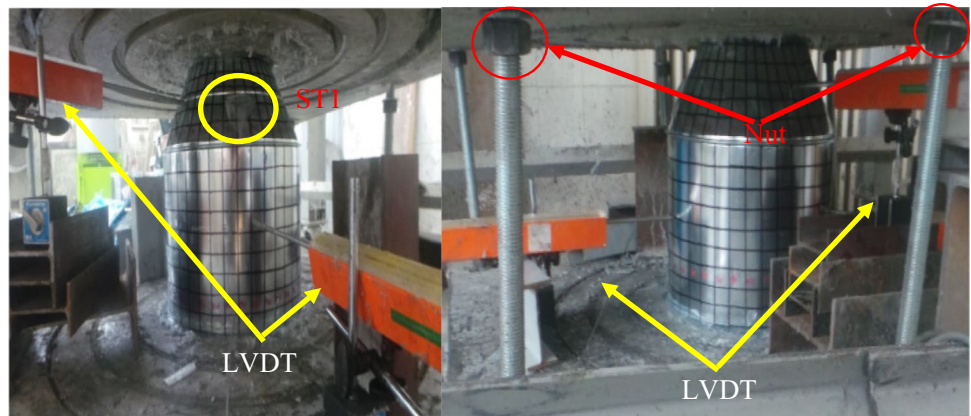


Table 2 Locations of strain gauges

Specimen	Strain gauges	
	S1°	S2°
Perfect model	270	10
4t	270	20
6t	270	–
8t	270	10
10t	270	10
14t	270	10
24t	270	10

S1=horizontal strain gauge on the cylindrical shell at 200 mm, and S2=vertical strain gauge on the conical shell at 100 mm

### 3 Test Results

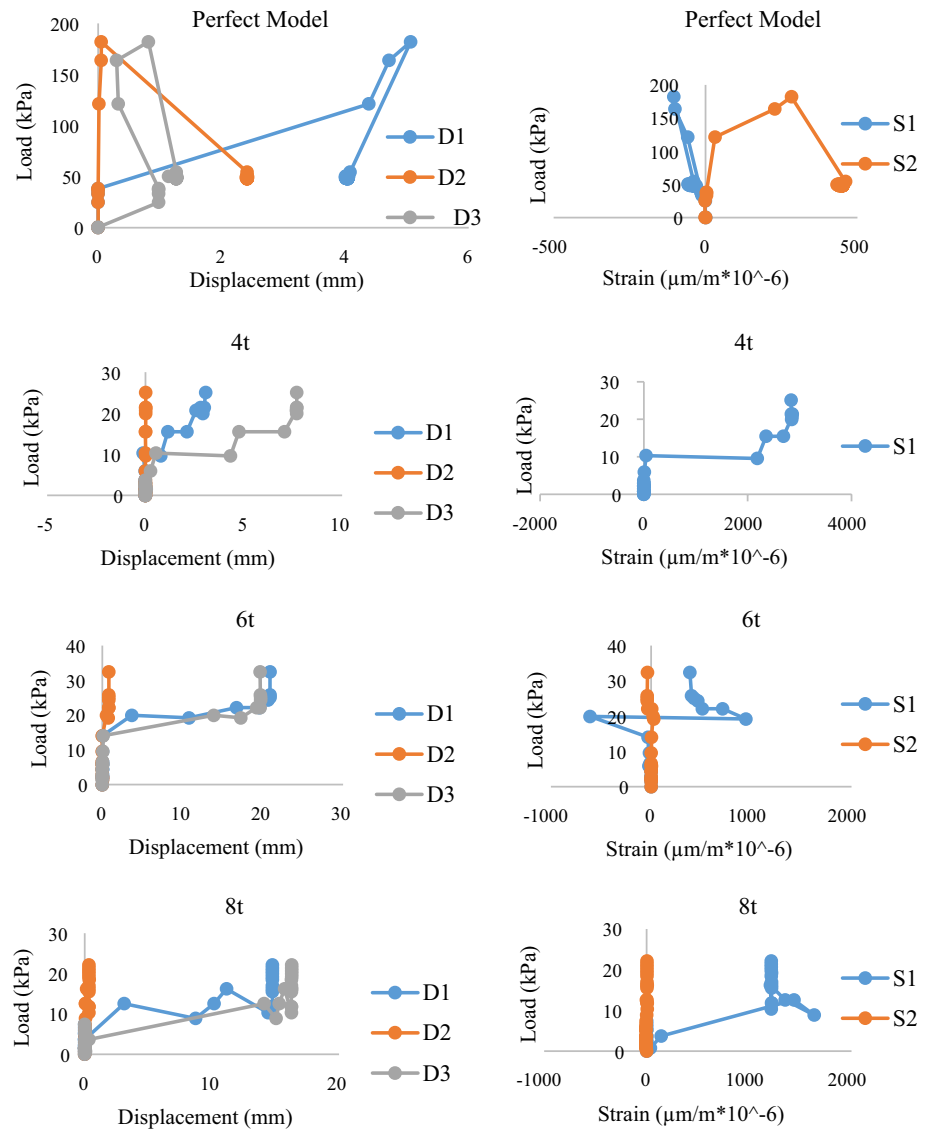
Figure 4 presents all of the load–strain and load–total displacement curves. The initial buckling (first buckling of the tanks), overall buckling (after initial buckling, all waves appeared to tanks), and collapse of all models (collapse load after the forms of V-shapes on the cylindrical section and bottom edges appeared) are given in Table 3. Before the initial buckling, the cylindrical shell was steady, and the edges of all tests were held in the radial direction. Every break represents one or more waves in these load-total displacement curves. There was good coordination between the LVDTs and strain gauge plots. Thus, this indicates the accuracy of the tests. Figure 4 shows that the horizontal strains acted the same as the vertical strains.

Table 4 presents the buckling loads of the specimens' tests. Table 4 demonstrates that subsequent buckling occurs after initial buckling, which is called the postbuckling effect. Alternately, the experimental models show resistance after initial buckling, which is a phenomenon

observed in all specimen tests. The overall buckling load was approximately 33–79% of the initial buckling load, and the collapse load was approximately 50–86% of the initial buckling load. Furthermore, the initial buckling load increased with increased dent depth and width.

Initial buckling is the most important phenomenon in thin-walled shells. Figure 5 demonstrates a comparison of the initial, overall and collapse buckling loads obtained from the specimens' tests. If compared the perfect model with the other test models according to Table 3, for perfect model initial buckling load and the 4t, 6t, 8t, and 10t experimental tests models, it can be said that this decreased by 142.01, 78.44, 277.07, 28.27, and 384.49%, respectively. In general, the initial buckling load decreased with increased the dent depth of the 4t–10t. on the other hand, if compared the perfect model with the other test models according to Table 3, for perfect model initial buckling load and the 14t, and 24t experimental tests models, it can be said that this increased by 51.76, and 79.74%, respectively. So, the experiments are compared with perfect-model dent applications made up to 10t emerge as defects. When the 14t and 24t experiments are considered, this situation stands out as reinforcement. As a result, for initial buckling, dents can be used for strengthening after 10t. If compared the perfect model with the other test models according to Table 3, for perfect model overall buckling load and the 4t, 6t, 8t, 10t and 14t experimental tests models, it can be said that this decreased by 683.53, 448.33, 647.78, 467.30, and 1.67%, respectively. In general, the overall buckling load decreased with increased the dent depth of the 4t to 14t. but, But, in the 14t test specimen decreased a little and this could be taken to zero. on the other hand, if compared the perfect model with the other test models according to Table 3, for perfect model overall buckling load and the 24t experimental tests models, it can be said that this increased by 47.14%. also, If compared the perfect model with the other test models according to Table 3,

**Fig. 4** Load–total displacement and load–strain curves for all experimental tests



for perfect model collapse buckling load and the 4t, 6t, 8t, 10t and 14t experimental tests models, it can be said that this decreased by 625.84, 460.94, 723.02, 473.85, and 19.09%, respectively. In general, the collapse buckling load decreased with increased the dent depth of the 4t to 14t. but, But, in the 14t test specimen decreased a little and this could be taken to zero. on the other hand, if compared the perfect model with the other test models according to Table 3, for perfect model collapse buckling load and the 24t experimental tests models, it can be said that this increased by 26.85%. Overall buckling and collapse buckling were examined; there was a decrease in buckling rates until the 14t experiment. However, in the 14t experiment, this drop rate was small, so overall buckling decreased by 1.67% and collapse buckling decreased by 19%.

This can be used instead of dent reinforcement because the drop rate is low. As a result, the dent used in 14t and 24t experiments can be used for strengthening purposes. Thus, the deeper the dent is, the more dent will behave like a stiffener.

#### 4 Theoretical Approximation

Jawad (2012) developed a theory to approximate the critical buckling load of thin-walled steel cones in 1980. The presented formulation was for an ideal geometric form as follows:

$$P_{cr} = 0.92E \left( R/L_e (t_e/R)^{2.5} \right) \quad (1)$$

Fig. 4 (continued)

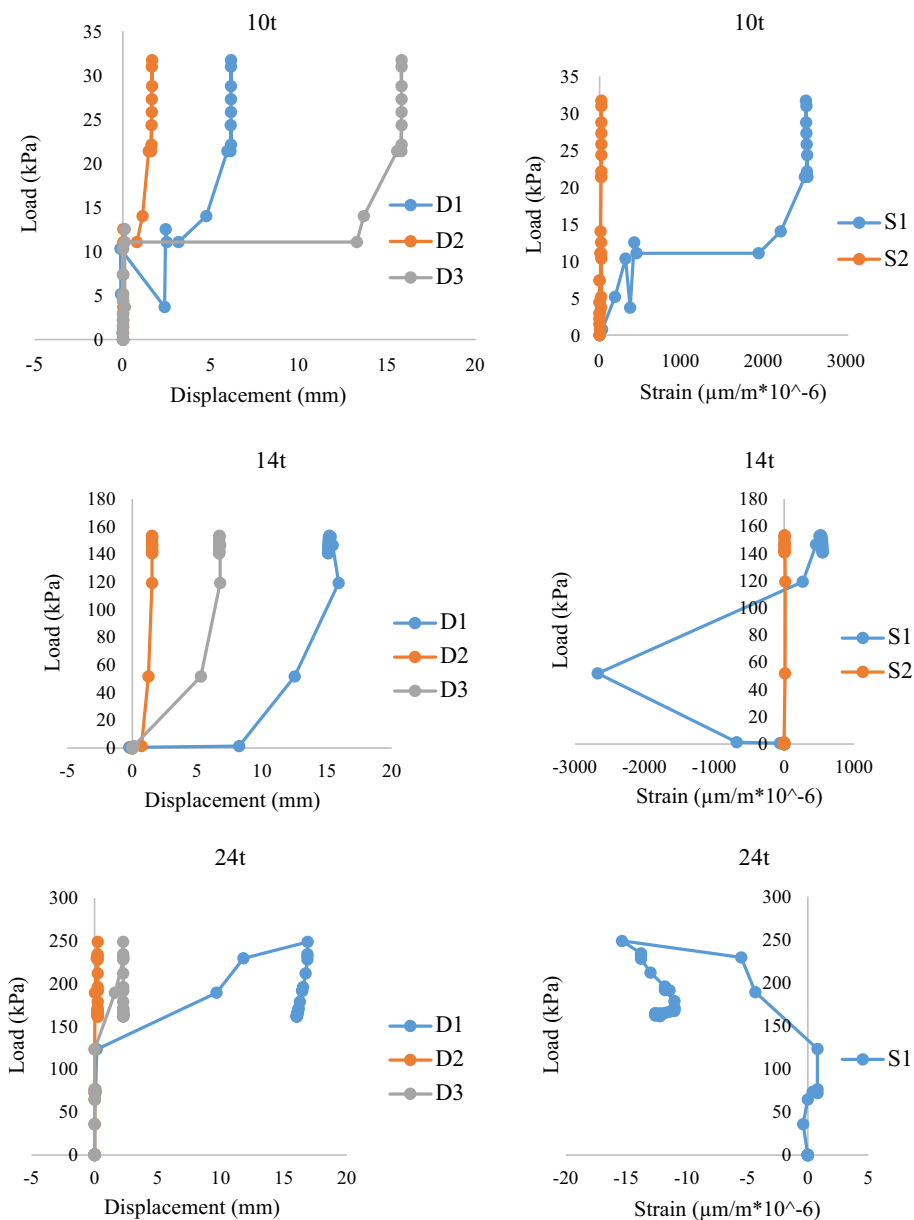


Table 3 The initial, overall, and collapse buckling of the models

Group	Initial buckling (kPa) $P_1$	Overall buckling (kPa) $P_2$	Collapse buckling (kPa) $P_3$	Experimental conical wave	Experimental cylindrical wave
Perfect model	25.00	121.29	181.97	4	8
4t	10.33	15.48	25.07	–	8
6t	14.01	22.12	32.44	–	7
8t	6.63	16.22	22.11	–	7
10t	5.16	21.38	31.71	–	7
14t	51.83	119.30	152.80	–	7
24t	123.42	229.45	248.77	–	7

where  $t$  is the thickness of the cone wall;  $t_e$  is the effective thickness of the cone and is equivalent to  $t \cdot \cos \alpha$ , where  $\alpha$  is the semi vertex angle of the cone;  $E$  is the Young's

modulus; and  $L_e$  is the effective length of the cone, found by  $L/2(1 + r/R)$ , in which  $L$  is the height of the cone,  $R$  is the lower radius, and  $r$  is the upper radius.

**Table 4** The buckling load comparison

Model	$(P_2 - P_1)/P_2$ (%)	$(P_3 - P_1)/P_3$ (%)	$(P_1 - \text{perfect model } P_1)/P_1$ (%)	$(P_2 - \text{perfect model } P_2)/P_2$ (%)	$(P_3 - \text{perfect model } P_3)/P_3$ (%)
Perfect model	79.39	86.26	–	0.00	0.00
4t	33.27	58.80	–142.01	–683.53	–625.85
6t	36.66	56.81	–78.44	–448.33	–460.94
8t	59.12	70.01	–277.07	–647.78	–723.02
10t	75.87	83.73	–384.50	–467.31	–473.86
14t	56.55	66.08	51.77	–1.67	–19.09
24t	46.21	50.39	79.74	47.14	26.85

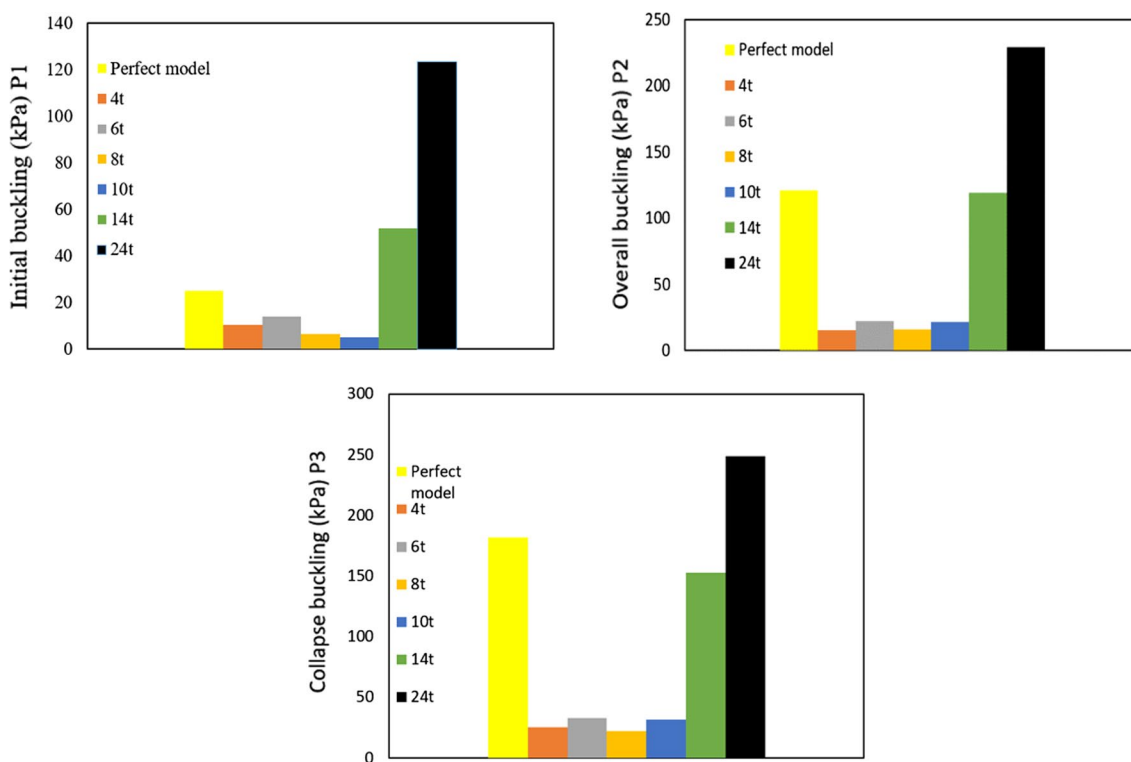


**Fig. 5** Comparison of the initial buckling load, overall buckling load and collapse load

**Table 5** The Jawad results for the models

Model	Jawad eq KPa	$P_1$ (KPa)	% to initial	$P_2$ (KPa)	% to overall	$P_3$ (KPa)	% to collapse
Perfect model	5.15	25.00	385.43	121.29	2255.12	181.97	3433.39
4t	–	10.33	100.58	15.48	200.54	25.07	386.79
6t	–	14.01	172.03	22.12	329.52	32.44	529.90
8t	–	6.63	28.74	16.22	214.951	22.11	329.3
10t	–	5.16	0.194	21.38	315.15	31.71	515.728
14t	–	51.83	906.41	119.30	2216.5	152.80	2866.99
24t	–	123.42	2296.50	229.45	4355.34	248.77	4730.4

Table 5 lists the buckling load values obtained from Jawad and compares them with the buckling loads of all specimens' tests. Figure 5 presents a comparison of the initial, overall, and collapse buckling loads obtained from specimen tests with the Jawad equation. The following results are obtained by looking at Fig. 5:

- The initial buckling load was approximately 1%-2297% the buckling load estimated based on the theories of Jawad,
- The overall buckling load was approximately 215%-4355% compared to the theories of Jawad estimates,
- The collapse load was approximately 330%-4730% compared to the theories of Jawad estimates.

In general, initial buckling is the most important phenomenon in thin-walled shells. Thus, if considering the buckling load estimated based on theory (Jawad), the elicited values are far smaller than the initial buckling load measured during the experiments. Also, The Jawad theory is only for conical structures and in this research, the conical structure we tested is with the cylindrical structure, so these differences may arise. However, the result is equal for the 10t test model in the initial buckling. In addition, it was far smaller than the overall and collapse loads measured during the experiments Fig. 6.

## 5 Collapse Mode

Table 3 gives the number of waves observed during the tests. The number of cylindrical waves obtained from the perfect models was 4 more than the number of waves obtained from the conical section. However, by creating dents, no waves were seen in the cone. In addition, it can be observed that the number of cylindrical waves observed from the tests decreased with increased dent depth and width. In contrast, Fig. 7 shows the effects of collapse of the waves. The collapse in all model tests is in the form of V-shapes on the cylindrical section and bottom edges. In addition, the wavelengths of the waves were equally observed in all models. The failure sound was very loud and scary in the 14t and 24t test models. Therefore, it can be observed that the depth of waves increased with increasing dent depth and width. Additionally, Fig. 7 clearly shows instances when the waves have the same length. In contrast, at the time of the creation of the first waves in all of the strain load diagrams, these waves were in elastic states. However, after entering the phases, the plastic stage was attained. Figure 7 shows all models before and after tests.

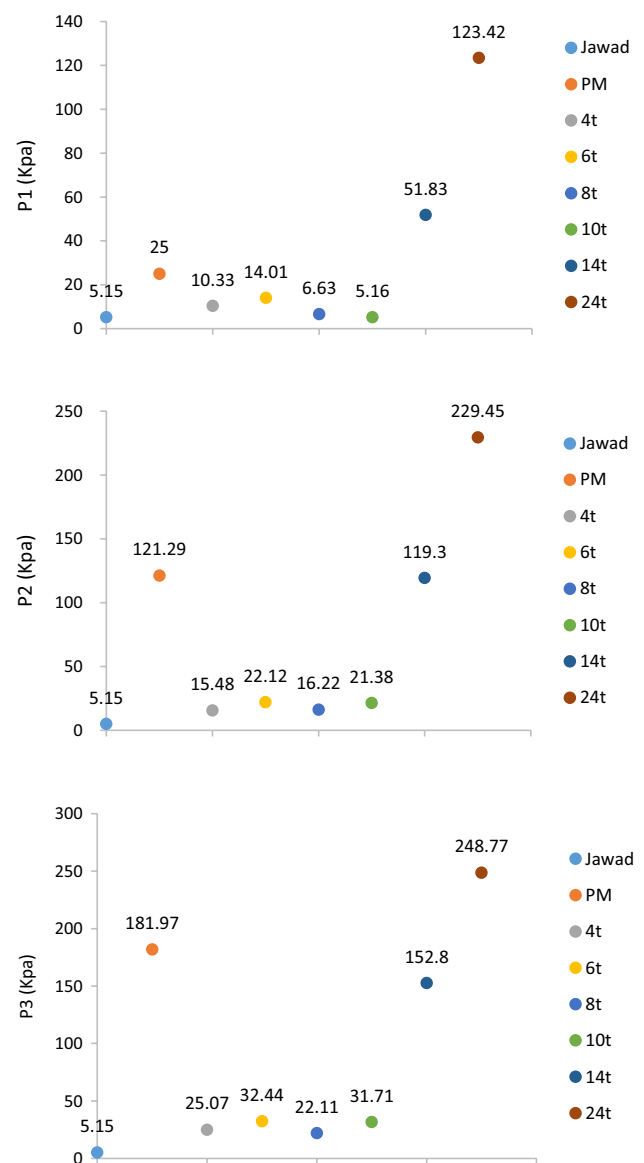


Fig. 6 Comparison of the Jawad equation with the initial buckling, overall buckling and collapse loads

## 6 Geometrical Imperfections Within the Standards

Authentic international codes for designing thin-walled shells, such as EuroCode-3 (2007), ECCS (2008) and DIN18800-4 (1990), simply limit the permitted deformations and disturbances in welding and construction of the thin-walled shells. The results are seen in Table 6.

However, different forms from different references (DIN18800-4, 1990; EuroCode-3, 2007; ECCS, 2008) for measuring the size of the initial depth of the dent on the wall of the shells in the longitudinal direction are represented here:



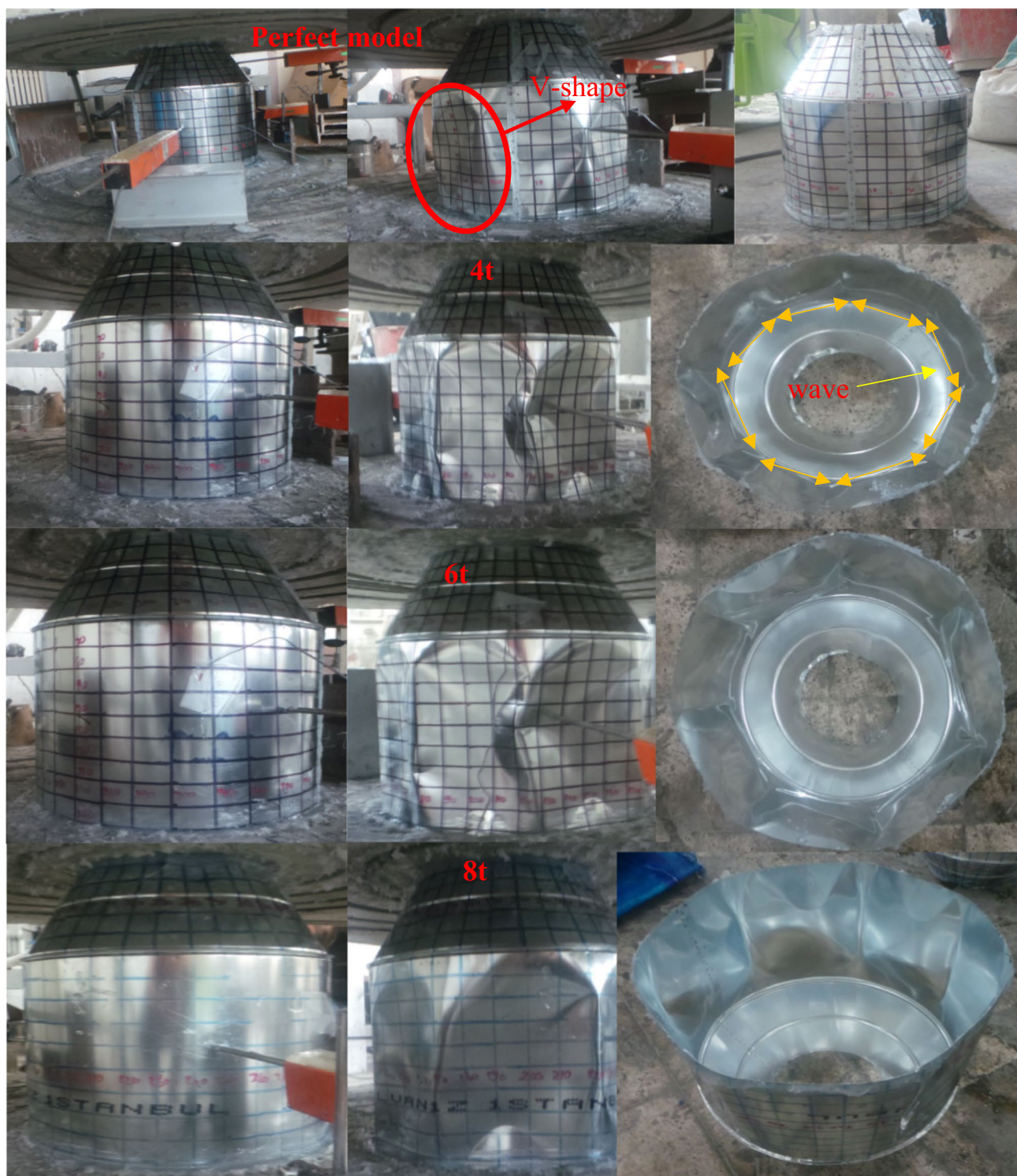


Fig. 7 Failure of the waves

$l_g = 4(r/t)^{0.5}$   
 $l_g = 25t \leq 500 \text{ mm}$  at welds for prENV 1993–1-6 (2007):  
 Eurocode 3.  
 $l_r = 4(r/t)^{0.5} \leq 0.95$  times the distance of the welds.

$l_r = 25t$  at welds for ECCS (2008).  
 $l_{mx} = 4(r/t)^{0.5} \leq 2000 \text{ mm}$ .  
 $l_{mx} \leq 500 \text{ mm}$  at welds for DIN 18,800.

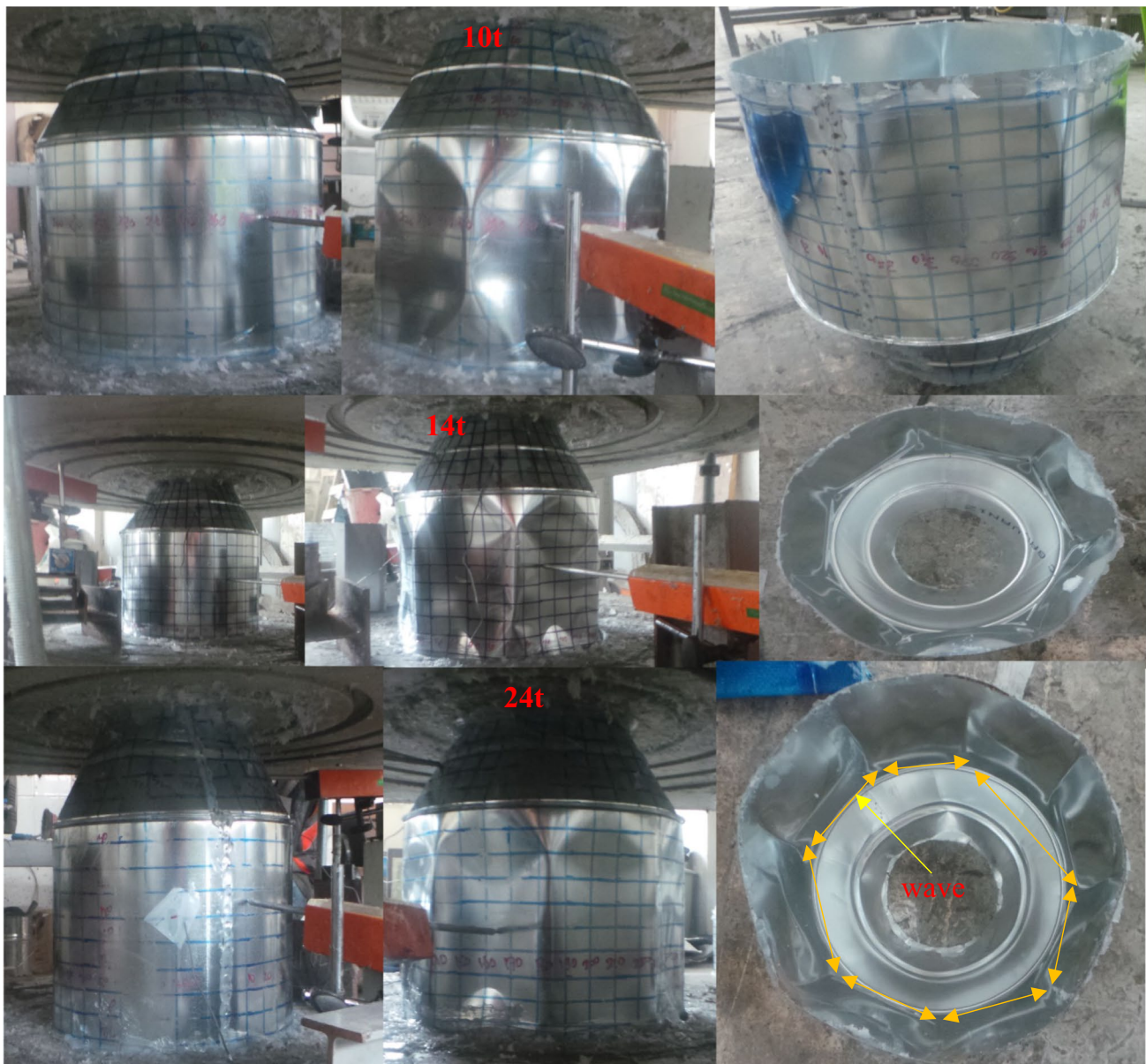
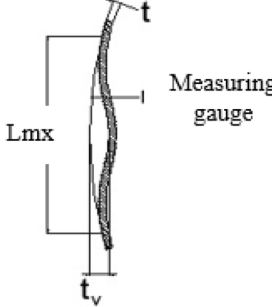
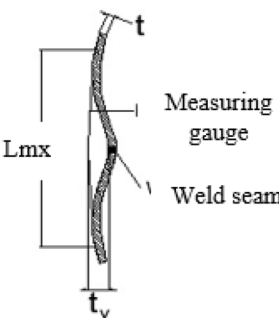


Fig. 7 (continued)

where  $t$  is the thickness of the cone,  $r$  is the middle surface of the shell and the cylinder shell, and  $l_{mx}$ ,  $l_r$  and  $l_g$  are the longitudinal imperfections created circumferentially. Table 6 is the exact place of this length. Because the size of the dent  $t_v$  and the length of the curve  $l_{mx}$  were designed and created with precise tools, there is no need to compute the limitation of the abovementioned formulas, and the  $t_v$  of specimens 4t, 6t, 8t, 10t, 14t and 24t ( $t$  is the thickness of the shell) was 1.8 mm, 2.7 mm, 3.6 mm, 4.5 mm, 6.3 mm, and 10.8 mm, respectively. The  $l_{mx}$  values of the 4t, 6t, 8t, 10t, 14t, and 24t samples were 1.8 mm, 2.7 mm, 3.6 mm, 4.5 mm, 6.3 mm, and 10.8 mm, respectively. The computation of  $t_v$  and  $l_{mx}$  reveals that their amount in all specimens

was much more than the amounts allowed by codes; thus, the obtained values are beyond the numbers permitted by codes. In such cases, the structure cannot be used. However, in the laboratory results for the 14t and 24t specimens, the initial buckling exceeded the initial buckling of the perfect specimen except for 24t, inducing a strengthening effect, which means that there is no need to take the structure out of use. In the case of other specimens, it should be noted that, although the initial buckling of this specimen was less than the amount for the perfect specimen, its postbuckling capacity was 2 times greater than the initial buckling, which means that there is no problem with using the structure. Probing the codes related to thin-walled shells shows that

**Table 6** Tolerances within the relevant standards

	Definition of the depth of initial dimples	Tolerances according to different standards
Depth of initial dimples in plates measured in vertical direction		DIN 18800-4 $t_v \leq 1\%$ of measuring length $L_{mx}$ ESSCRec (2008) $L_{mx} = l_r \cdot t_v = w$ $t_v \leq 1\%$ of measuring length $L_{mx}$ pr ENV 1993-1-6 (2007) $L_{mx} = L_p \cdot t = w_0$ Class A: $T \leq 0,006 \cdot L_{mx}$ Class B: $T \leq 0,010 \cdot L_{mx}$ Class C: $T \leq 0,016 \cdot L_{mx}$
Initial dimple of circumferential weld seam		DIN 18800-4 $t_v \leq 1\%$ of measuring length $L_{mx}$ ESSCRec (2008) $L_{mx} = l_r \cdot t_v = w$ $t_v \leq 1\%$ of measuring length $L_{mx}$ pr ENV 1993-1-6 (2007) $L_{mx} = L_p \cdot t = w_0$ Class A: $T \leq 0,006 \cdot L_{mx}$ Class B: $T \leq 0,010 \cdot L_{mx}$ Class C: $T \leq 0,016 \cdot L_{mx}$

$L_{mx} = 25 \leq 500$  mm

there is no case referring to postbuckling capacities of this size. They simply suggest they not be used, and this requires a great deal of investigation and thought.

## 7 Conclusions

The present study focused on the buckling of nose cone-type steel thin-walled shells. Experimental investigation of seven specimens with simple supports and different imperfections under hydrostatic pressure reveals the following:

- After the initial buckling, the models resisted postbuckling behavior. Then, the models presented postbuckling behavior.
- The initial buckling is increased with increased dent width and depth.
- The imperfect models are compared with the perfect one, and dent applications made up to  $10t$  emerge as defects. When the 14t and 24t experiments are considered, this situation stands out as reinforcement. As a result, for initial buckling, dents can be used for strengthening after  $10t$ .
- The overall buckling and collapse buckling were examined; there was a decrease in buckling rates until the 14t experiment. However, in the 14t experiment, this drop rate was small, so overall buckling decreased by 1.67% and collapse buckling decreased by 19%. This can be used instead of dent reinforcement because the drop rate is low. As a result, the dent used in 14t and 24t experiments can be used for strengthening purposes.
- The observed initial buckling load was approximately 1%-2297% the buckling load estimated based on the theories of Jawad, and the overall buckling load was approximately 215%-4355% compared to the theories of Jawad estimates. The collapse load was approximately 330%-4730% compared to the theories of Jawad estimates. In general, we can assume that, if we consider the buckling load estimated based on theory (Jawad), the elicited values are far smaller than the initial buckling load measured during the experiments.
- The experimental number of waves was shown. The number of cylindrical waves obtained from the perfect models was four more than the number of waves obtained from the conical section. However, by creating dents, no waves were seen in the cone.
- The collapse in all model tests is in the form of V-shapes on the cylindrical section. In addition, the wavelengths of the waves were equally observed in all models. Therefore, it can be observed that the depth of waves increased with increasing dent depth and width.
- The results of the present work revealed that, despite the regulations of international codes, geometric imperfec-

tions are not always bad for the structures, and the regulations are in urgent need of revision.

## References

- Aghajari, S., Abedi, K., & Showkati, H. (2006). Buckling and post-buckling behavior of thin-walled cylindrical steel shells with varying thickness subjected to uniform external pressure. *Thin Walled Structures*, *44*, 904–909.
- DIN 18800: (1990). Stahlbauten; Teil 4: Stabilitätsfalle, Schalenbeulen.
- ECCS EDR5. (2008). European Recommendations for Steel Construction: Buckling of Shells, 5th edition, Edited by J.M. Rotter and H. Schmidt, European Convention for Constructional Steelwork, Brussels, 384 pp.
- EN-1993-1-6 : Eurocode 3: (2007). Design of steel structures, Part 1.6: General rules- Strength and stability of shell structures, Eurocode 3 Part 1.6, CEN, Brussels.
- Fatemi, S. M., Showkati, H., & Maali, M. (2013). Experiments on imperfect cylindrical shells under uniform external pressure. *Thin Walled Structures*, *65*, 14–25.
- Ghazijahani, T. G., Dizaji, S. H., Nozohor, J., & Zirakian, T. (2015). Experiments on corrugated thin cylindrical shells under uniform external pressure. *Ocean Engineering*, *106*, 68–76.
- Ghazijahani, T. G., Jiao, H., & Holloway, D. (2014a). Influence of a cutout on circular steel hollow sections under cyclic loading. *Journal of Construction Steel Research*, *100*, 12–20.
- Ghazijahani, T. G., Jiao, H., & Holloway, D. (2014b). An experimental study on externally pressurized stiffened and thickened cylindrical shells. *Thin Walled Structures*, *85*, 359–366.
- Ghazijahani, T. G., Jiao, H., & Holloway, D. (2014c). Experiments on dented cylindrical shells under peripheral pressure. *Thin-Walled Structures*, *84*, 50–58.
- Ghazijahani, T. G., Jiao, H., & Holloway, D. (2015a). Structural behavior of shells with different cutouts under compression: An experimental study. *Journal of Construction Steel Research*, *105*, 129–137.
- Ghazijahani, T. G., Jiao, H., & Holloway, D. (2015b). Timber filled CFRP jacketed circular steel tubes under axial compression. *Construction and Building Materials*, *94*, 791–799.
- Ghazijahani, T. G., & Showkati, H. (2011). Experiments on conical shell reducers under uniform external pressure. *Journal of Construction Steel Research*, *67*, 1506–1515.
- Ghazijahani, T. G., & Zirakian, T. (2014). Determination of buckling loads of conical shells using extrapolation techniques. *Thin Walled Structures*, *74*, 292–299.
- Golzan, B. S., & Showkati, H. (2008). Buckling of thin-walled conical shells under uniform external pressure. *Thin-Walled Structures*, *46*, 516–529.
- Jawad, M. H. (2012). Theory and design of plate and shell structures. Chapman & Hall, Inc;344.
- Maali, M., Kılıç, M., Yaman, Z., Ağcakoca, E., & Aydın, A. C. (2019). Buckling and post-buckling behavior of various dented cylindrical shells using cfrp strips subjected to uniform external pressure: comparison of theoretical and experimental data. *Thin Walled Structures*, *137*, 29–39.
- Maali, M., Showkati, H., & Fatemi, M. S. (2012). Investigation of the buckling behavior of conical shells under weld-induced imperfections. *Thin Walled Structures*, *57*, 13–24.
- Niloufari, A., Showkati, H., Maali, M., & Fatemi, M. S. (2014). Experimental investigation on the effect of geometric imperfections on the buckling and post-buckling behavior of steel tanks under hydrostatic pressure. *Thin Walled Structures*, *74*, 59–69.
- Sagiroglu, M. (2018). Experimental evaluation of the post-fire behavior of steel T-component in the beam-to-column connection. *Fire Safety Journal*, *96*, 153–164.
- Showkati, H., & Ansourian, P. (1996). Influence of primary boundary conditions on the buckling of shallow cylindrical shells. *Journal of Construction Steel Research*, *3*, 53–75.
- Showkati, H., & Shahandeh, R. (2009). Experiments on the buckling behavior of ring-stiffened pipelines under hydrostatic pressure. *Journal of Engineering Mechanics*, *136*, 464–471.

**Publisher's Note** Springer Nature remains neutral with regard to jurisdictional claims in published maps and institutional affiliations.